Theoretical Study of the Reaction of Si^+ with C_3H_2

Pilar Redondo, Ana Sagüillo, Carmen Barrientos, and Antonio Largo*

Departamento de Química Física, Facultad de Ciencias, Universidad de Valladolid, 47005 Valladolid, Spain

Received: November 9, 1998; In Final Form: February 18, 1999

A theoretical study of the $(SiC_3H)^+$ and $(SiC_3H_2)^+$ species has been carried out. Two different models, MP4 at MP2 geometries and QCISD(T) at B3LYP geometries, have been employed. Significant differences are encountered when spin contamination is relatively high. Our calculations predict that the global minimum of the $(SiC_3H)^+$ system is a cyclic isomer, derived from protonation of the SiC_3 ground state. The proton affinities of the three lowest-lying isomers of SiC_3 have been computed, obtaining relatively high values in all cases. The lowest-lying $(SiC_3H_2)^+$ species has a linear carbon backbone and can be formally derived from the bonding of Si^+ to vinylidenecarbene (l-C_3H_2) through an electron lone pair. The cyclic isomer obtained from cyclopropenylidene (c-C_3H_2) is also quite stable, lying only about 9−12 kcal/mol above the ground state. For the reaction of Si^+ with c-C_3H_2, charge transfer is endothermic, whereas production of SiC_3^+ is slightly exothermic and exhibits a small barrier. The preferred channel is formation of cyclic SiC_3H^+, since it is clearly exothermic and barrier-free. In the case of the reaction of Si^+ + l-C_3H_2 charge transfer is also endothermic and the path leading to linear SiC_3^+ involves a high energy barrier. There are two possible competitive processes which are barrier-free: production of linear SiC_3H^+ and formation of cyclic SiC_3H^+ through a previous isomerization into a cyclic $SiC_3H_2^+$ species. Therefore, the reactions of Si^+ with both c-C_3H_2 and l-C_3H_2 are feasible in the interstellar medium and consequently possible sources of precursors of SiC_3.

Introduction

Binary silicon carbides have received much attention in recent years. In addition to their interest in microelectronics,[1] small binary silicon−carbon clusters are relevant in astrophysics. So far SiC,[2] SiC_2,[3] and SiC_4[4] have been detected in space. These silicon carbides are strongly related to the family of organosulfur compounds SC_x, in which case SC_2[5] and SC_3[6] have been observed in the interstellar medium. Therefore, SiC_3 seems a good candidate for detection in space. A theoretical study by Alberts et al.[7] predicts a rhomboidal structure, with a transannular carbon−carbon bond, to be the ground state. Nevertheless, the linear isomer and a second rhomboidal structure with a carbon−silicon transannular bond lie only 4.1 and 4.3 kcal/mol, respectively, higher in energy according to the theoretical calculation. Consequently, there are in principle three different SiC_3 isomers that could be formed in space. Which of them is produced could depend on the synthetic route.

Given the conditions reigning in the interstellar medium, namely low density and low temperature, important reactions must be exothermic and have low (or zero) activation energy. Those are the main reasons for the importance of ion−molecule reactions in interstellar chemistry. In fact, binary silicon−carbon compounds have been proposed to be formed in the reaction of Si^+ with hydrocarbons.[8] In particular, both experimental[9,10] and theoretical studies[11] have shown that SiC_2 could be produced through a synthetic route initiated by the reaction of Si^+ with acetylene. A similar reaction scheme may be proposed for the production of SiC_3. In first place the reaction of Si^+ with C_3H_2 may lead to the protonated form of SiC_3, and subsequent dissociative recombination could finally produce SiC_3:

$$Si^+ + C_3H_2 \rightarrow SiC_3H^+ + H \quad (1)$$

$$SiC_3H^+ + e \rightarrow SiC_3 + H \quad (2)$$

Two different C_3H_2 isomers have been detected in the interstellar medium. Cyclopropenylidene, c-C_3H_2, was first observed in space several years ago[12] and is one of the most abundant interstellar hydrocarbons, as well as the first interstellar organic ring. Propadienylidene (singlet vinylidenecarbene), l-C_3H_2, was observed in space[13] more recently and has a linear carbon backbone and two hydrogens bonded to a terminal carbon atom. Theoretical studies[14,15] predict cyclopropenylidene to be the ground state, whereas vinylidenecarbene lies about 14 kcal/mol higher in energy. Experimental studies on these reactions are difficult to carry out, due to the difficulty in preparing C_3H_2 species. Therefore, theoretical studies could be particularly valuable in order to ascertain whether SiC_3 could be formed in space trough a reaction scheme involving the reaction of Si^+ with C_3H_2 species. In fact, we have carried out a similar study[16] in the case of the phosphorus analogue, C_3P, concluding that both cyclic and linear C_3P isomers could be produced in space.

In the present work, we have carried out a theoretical study of reaction 1, determining its energetics as well as characterizing the relevant transition states.This will allow a prediction not only of the reaction enthalpy, but also of possible activation barriers involved in the production of SiC_3H^+. Both C_3H_2 isomers, cyclic and linear, will be considered as reactants, since both are present in the interstellar medium. In first place, a study

* To whom correspondence should be addressed.

10.1021/jp984353k CCC: $18.00
Published on Web 04/13/1999

of the possible products, the $(SiC_3H)^+$ species, will be presented. Other possible products which may compete, like the SiC_3^+ species, have been theoretically studied in a previous work.[17]

Computational Methods

The geometries of the different species studied in the present work have been obtained at MP2 (second-order Møller−Plesset) level with the 6-31G* basis set.[18] In addition, for comparative purposes, density functional theory (DFT) was also employed for obtaining optimized geometries. For the DFT calculations we selected the B3LYP exchange-correlation functional[19] and the 6-311G** basis set[20] for carbon and hydrogen atoms and the McLean and Chandler basis set[21] (supplemented with a set of d functions) for silicon.

Harmonic vibrational frequencies have been computed on each optimized structure at its corresponding level of theory. This allows an assessment of the nature of stationary points, as well as an estimate of the zero-point vibrational energy (ZPVE) correction. In order to compute the ZPVE values at the MP2 level, the corresponding vibrational frequencies were scaled by a factor of 0.94.

On the MP2/6-31G* geometries, single-point calculations at the fourth-order Møllet−Plesset (MP4) level[22,23] were carried out in order to compute electronic energies. In the case of B3LYP geometries we performed subsequent single-point calculations at the QCISD(T) level,[24] which stands for a quadratic CI calculation with singles and doubles substitutions followed by a perturbative treatment of triple substitutions. In both cases, MP4 and QCISD(T), we employed the 6-311G** basis set and the frozen-core approximation (inner-shell orbitals were not included for computing electron correlation energies). We must recall that in our previous study[17] on SiC_3^+, QCISD(T)/6-311G** calculations on B3LYP geometries were shown to provide very similar results to the most expensive CCSD(T)/cc-pVTZ//B3LYp/cc-pVTZ level. Therefore, QCISD(T)/6-311G** seems a reasonable compromise between cost and quality for these systems.

All calculations were carried out with the Gaussian-94 program package.[25]

Results and Discussion

$(SiC_3H)^+$ Isomers. We have found several $(SiC_3H)^+$ isomers, in both their singlet and triplet states, but we will only present the results for those which are more stable. The geometrical parameters of 14 $(SiC_3H)^+$ species are shown in Figure 1, and the corresponding relative energies at different levels of theory are given in Table 1 (PMP4 stands for projected MP4 values). For comparison purposes we give the relative energies of the lowest-lying isomers of SiC_3 in Table 2. All structures shown in Figure 1 are true minima, since all their vibrational frequencies are positive (the corresponding harmonic vibrational frequencies and IR intensities are available upon request).

Structures **1**−**6** are formally obtained from protonation of the corresponding singlet and triplet states of linear SiC_3, which can be schematically represented by the following valence bond structures:

$$^1\Delta \qquad :Si{=}C_1{=}C_2{=}C_3:$$

$$^3\Sigma^- \qquad :Si{-}C_1{=}C_2{=}C_3:$$

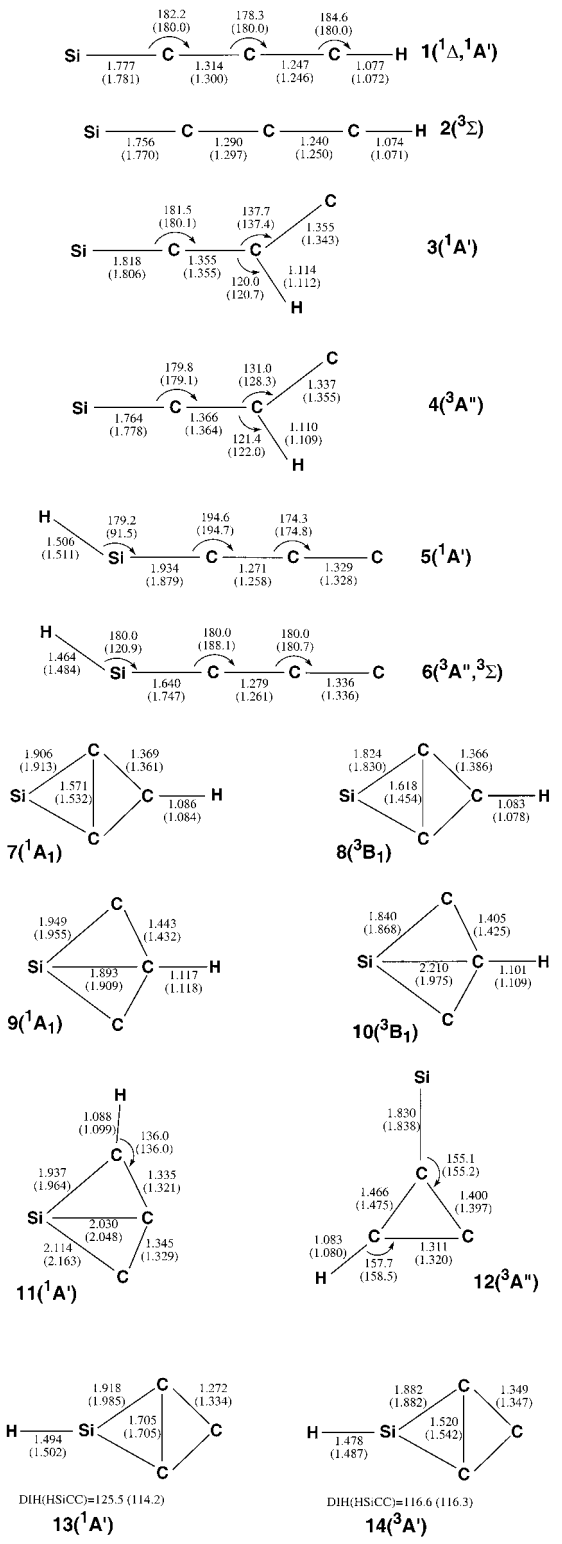

Figure 1. MP2/6-31G* and B3LYP/6-311G** (in parentheses) optimized geometries for the different SiC_3H^+ species. Distances are given in angstroms and angles in degrees.

Since the lowest-lying linear state of SiC_3 is a triplet[7] ($^3\Sigma^-$), triplet protonated species are also favored over the singlet ones when protonation takes place at a carbon atom (species **2** and **4**). On the other hand, when protonation takes place at silicon the stability order is reversed, since all theoretical levels agree in that structure **5** is lower in energy than **6**. As expected, protonation at carbon is preferred over protonation at silicon when both atoms have lone pairs. Therefore, the preferred protonation site is the terminal carbon atom (structures **1** and

TABLE 1: Relative Energies (kcal/mol) for the (SiC_3H^+) States at Different Levels of Theory with the 6-311G Basis Set[a]**

	1	2	3	4	5	6	7	8	9	10	11	12	13	14
MP2	27.9	21.1	114.7	88.4	73.7	102.2	0.0	57.4	91.2	68.3	26.0	43.9	78.8	73.8
MP4	21.7	14.4	102.0	78.5	61.6	95.0	0.0	59.6	85.3	63.6	21.5	41.7	71.4	74.6
PMP4	21.7	6.8	102.0	73.1	61.6	90.2	0.0	59.6	85.3	58.3	21.5	40.1	71.4	73.3
B3LYP	11.2	−7.7	88.2	57.0	58.3	65.1	0.0	53.6	88.3	52.9	18.7	29.8	80.4	69.5
QCISD(T)	20.4	4.2	91.4	64.8	62.4	74.0	0.0	57.1	86.2	57.1	20.5	36.8	70.4	71.5
ZPVE (MP2)	12.40	12.60	11.51	12.20	10.48	11.44	14.01	13.96	12.28	13.43	13.32	13.48	12.01	12.30
ZPVE (B3LYP)	13.95	13.75	12.43	12.20	10.67	10.94	14.57	13.53	11.66	13.28	13.76	13.97	11.02	12.37

[a] Zero-point vibrational energy differences were obtained at the MP2=full/6-31G* level (MP2, MP4, and PMP4) or at the B3LYP/6-311G** level (B3LYP and QCISD(T)).

TABLE 2: Relative Energies (kcal/mol) for the Lowest-Lying Isomers of SiC_3 at Different Levels of Theory[a]

	linear SiC_3	rhomboidal SiC_3	
		C−C trans. bond	Si−C trans. bond
MP2	17.2	0.0	11.8
MP4	11.4	0.0	7.8
PMP4	8.0	0.0	7.8
B3LYP	−7.7	0.0	4.7
QCISD(T)	6.7	0.0	7.4
ZPVE (MP2)	6.90	6.72	6.59
ZPVE (B3LYP)	7.17	6.84	6.63

[a] ZPVE differences were obtained at the MP2=full/6-31G* level (MP2, MP4, PMP4), or at the B3LYP/6-311G** level (B3LYP, QCISD(T)).

2). Nevertheless, protonation at C_2 is not always preferred over protonation at silicon, since structure **3** is less stable than **5**, and **4** lies only about 8−17 kcal/mol below **6** depending on the level of calculation. We have also obtained the corresponding singlet and triplet species derived from protonation at C_1, but they have similar relative energies than **3** and **4** (lying about 1 kcal/mol higher at the B3LYP level). All other structures with silicon in a central position of the carbon chain are even less stable and are not presented in this work for the sake of space.

It is interesting to point out that structure **1** is only linear at the B3LYP level, whereas at the MP2 level it is slightly bent. Forcing linearity at the MP2 level results in an imaginary frequency (92i cm^{-1}) associated to HCC bending (of course a $^1\Delta$ state requires two determinants for its proper description). Nevertheless, the relative energy of this species at the MP4 level differs only in 10 kcal/mol with the corresponding B3LYP value. On the other hand, a much more dramatic change is observed in the case of structure **6**. In this case the MP2 level predicts a linear arrangement, whereas the molecule is nonlinear at the B3LYP level.

Structures **7** and **8** are the singlet and triplet protonated species derived from the most stable rhomboidal SiC_3 isomer,[7] with a transannular carbon−carbon bond. Structures **9** and **10** are the corresponding protonated derivatives obtained from the second SiC_3 four-membered ring with transannular silicon−carbon bond,[7] whereas structure **11** is the result of protonation at a terminal carbon atom of the singlet species. We did not find the corresponding triplet isomer in this case, since our attempts of optimization led to structure **2**. This is not surprising since a topological analysis of the electron density in terms of Bader's theory[26] carried out by Sudhakar and Lammertsma[27] shows that in fact the parent SiC_3 isomer has a T-shape structure in its singlet state, whereas we have found that the triplet SiC_3 species has a truly four-membered ring structure with peripheral Si−C bonds. Therefore, in the case of the singlet state the noncentral carbon atoms have lone pairs and are preferred protonation sites, resulting in structure **11** which is much more stable (about 66 kcal/mol at the QCISD(T) level) than structure **9** which is obtained upon protonation at central carbon where no lone pairs exist.

Structure **12** can be formally derived from a three-membered ring of SiC_3, which was found by Alberts et al.[7] to lie about 36 kcal/mol above the ground state. In this case we only present the triplet state, since all attempts to obtain an optimized structure for the singlet state led to structure **7**.

Finally, structures **13** and **14** are the singlet and triplet states obtained upon protonation at silicon of the corresponding states of the most stable rhomboidal SiC_3 isomer. Again, protonation at the carbon atom is preferred over protonation at silicon for cyclic species, since both **13** and **14** lie much higher than the corresponding protonated structures at carbon (structures **7** and **8**).

Concerning the relative energies shown in Table 1 it is generally observed that there are no large discrepancies between the Møller−Plesset values and the QCISD(T) ones. The largest discrepancy is noted for isomer **6** and can be mainly ascribed to the differences in the MP2 and B3LYP geometries in this case. In most cases (with the exception of **3**, **4**, and **6**) the difference between relative energies computed at the PMP4 and QCISD(T) levels is smaller than 3 kcal/mol. On the other hand the largest discrepancies are observed between the B3LYP values and ab initio relative energies. The worst case is again structure **6**, because of the rather different geometrical parameters obtained at the B3LYP level. Nevertheless, this is one of the less stable structures. More significant is the discrepancy between B3LYP and ab initio values for the relative energy of the triplet linear isomer **2**. Whereas at the PMP4 and QCISD(T) levels the energy difference between structures **2** and **7** virtually reproduces the relative energy of the parent linear and cyclic SiC_3 linear isomers (see the values in Table 2), the stability order is reversed at the B3LYP level, with the linear protonated species lying 7.7 kcal/mol below the cyclic one. This is the most important qualitative difference between B3LYP and ab initio results for the $(SiC_3H)^+$ isomers, since a different global minimum is predicted. Nevertheless, we believe that most likely the ab initio results are more reliable in this case, since correlation effects are very important in those cases where three- or four-membered rings are competing with noncyclic structures. The coincidence in the relative energies of two models like QCISD(T) and projected MP4 provides further support for this assertion. Furthemore, it is worth pointing out that at the HF/6-311G** level the linear triplet structure lies more than 21 kcal/mol below structure **7**. Therefore, the B3LYP result seems to be halfway between Hartree−Fock and correlated values. The anomalous behavior of B3LYP for computing the relative energy of the cyclic and linear isomers of $(SiC_3H)^+$ is also observed for the parent neutral molecule. Whereas for SiC_3 both MP4 and QCISD(T) relative energies are consistent with the results obtained by Alberts et al.,[7] at the B3LYP level the linear isomer

TABLE 3: Proton Affinities (kcal/mol) at Different Levels of Theory for the Lowest-Lying Isomers of SiC_3

	linear	rhomboidal SiC_3	
	SiC_3	C−C trans. bond	Si−C trans. bond
MP2	223.2	228.0	213.7
MP4	224.8	228.8	214.1
PMP4	232.3	228.8	214.1
B3LYP	228.0	228.9	214.9
QCISD(T)	229.9	228.2	215.2
ΔZPVE (MP2)	5.70	7.30	6.73
ΔZPVE (B3LYP)	6.58	7.73	6.91

is predicted to lie 8 kcal/mol below the cyclic isomer (see Table 2), nearly the same value obtained for $(SiC_3H)^+$.

Protonation of the third low-lying SiC_3 isomer, the four-membered ring with the transannular silicon−carbon bond which according to Alberts et al.[7] lies only about 4.3 kcal/mol above the SiC_3 ground state, results in less stable structures. We have already pointed out that protonation takes place preferentially at a terminal carbon atom, resulting in structure **11**. All theoretical methods agree in this case, since all predict an energy difference with the global minimum, structure **7**, around 20 kcal/mol. The most important difference observed for this structure, compared with the parent neutral isomer, is the lengthening of the silicon−central carbon distance (1.880 Å at correlated levels[7]). This means that upon protonation the silicon−carbon transanular bond is weakened, and this undoubtedly affects the stability of this structure.

The results for the $(SiC_3H)^+$ system allow an estimate of the proton affinity of SiC_3, which is an important property in gas phase chemistry and particularly in proton-rich interstellar media, where proton transfer reactions may play an important role. The proton affinity is computed as

$$PA(T) = -\Delta E_e - \Delta E_v - \Delta E_r + 5/2RT$$

where ΔE_e is the electronic energy difference, ΔE_v the vibrational energy difference (which can be taken as the zero-point vibrational energy difference), and ΔE_r the rotational energy difference for the reaction

$$SiC_3 + H^+ \rightarrow (SiC_3H)^+$$

We will only provide results for the PA of the three lowest-lying isomers of SiC_3, namely the four-membered ring with transannular carbon−carbon bond, the linear triplet isomer, and the rhomboidal species with transannular silicon−carbon bond. Furthermore, only values for protonation at the most favorable site will be provided; that is, only production of structures **7**, **2**, and **11** will be considered. The results at different levels of theory are shown in Table 3.

It can be readily seen that there is a very good agreement between the PA's at different levels of theory in all cases. The three SiC_3 isomers have very high proton affinities, and therefore could undergo protonation quite easily if they are present in proton-rich interstellar media. It is worth noting that the PAs of the SiC_3 ground state and the linear isomer are very similar at the most reliable levels of theory, whereas in the case of the second rhomboidal structure, where protonation takes place at a terminal carbon atom to give structure **11**, a somewhat lower PA is obtained.

$(SiC_3H_2)^+$ Isomers. Only the more relevant $(SiC_3H_2)^+$ species will be discussed. Therefore we will present stable structures on the doublet $(SiC_3H_2)^+$ surface, since the reaction of Si^+ with C_3H_2 will take place in principle on the doublet surface.

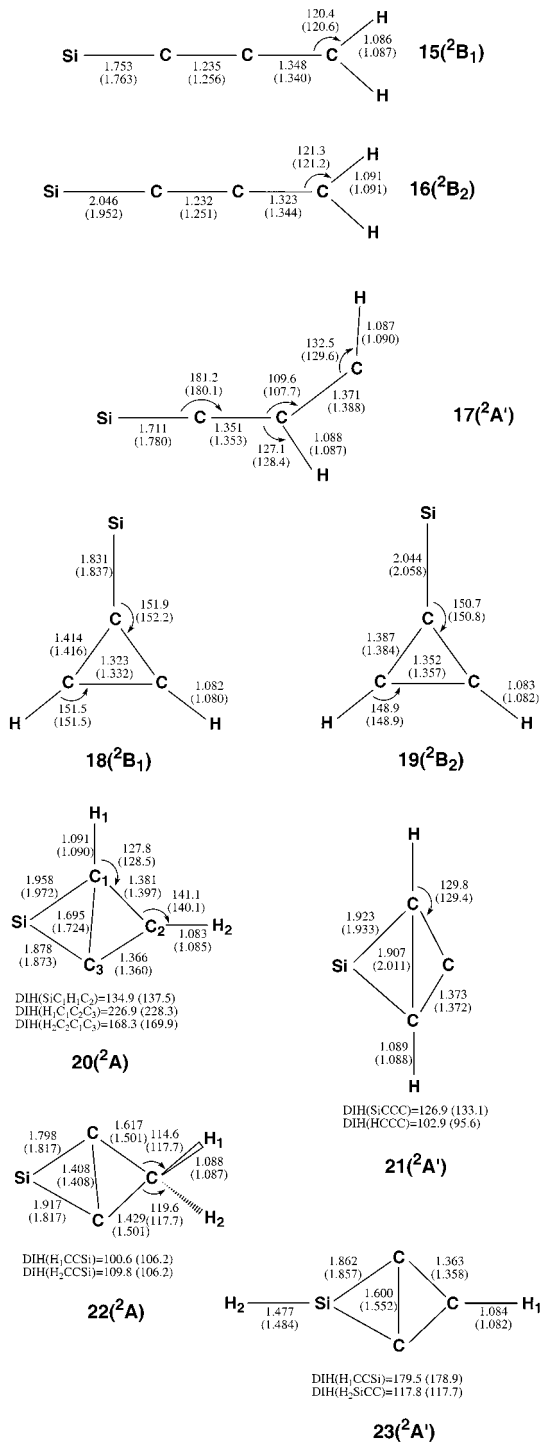

Figure 2. MP2/6-31G* and B3LYP/6-311G** (in parentheses) optimized geometries for the different $SiC_3H_2^+$ isomers. Distances are given in angstroms and angles in degrees.

The optimized geometries for the different $(SiC_3H_2)^+$ structures are shown in Figure 2, whereas their relative energies are given in Table 4. All structures are true minima on the $(SiC_3H_2)^+$ surface. The corresponding harmonic vibrational frequencies and IR intensities are provided as Supporting Information.

Structures **15** and **16** have linear carbon backbones and can be viewed as the result of the interaction of Si^+ with vinylidenecarbene (l-C_3H_2) through the end carbon. The corresponding electronic configurations are the following:

TABLE 4: Relative Energies (kcal/mol) for the $(SiC_3H_2)^+$ Species at Different Levels of Theory with the 6-311G Basis Set[a]**

	15	16	17	18	19	20	21	22	23
MP2	0.0	48.7	79.9	−1.4	14.3	21.8	28.4	40.4	30.0
MP4	0.0	47.1	77.7	2.8	18.6	24.4	31.0	43.3	37.0
PMP4	0.0	46.9	76.8	8.6	24.3	27.5	33.7	47.4	42.9
B3LYP	0.0	45.4	74.5	12.0	30.8	35.8	40.4	59.9	54.9
QCISD(T)	0.0	43.0	71.3	8.8	25.2	27.7	33.7	49.1	45.5
ZPVE (MP2)	20.59	20.35	20.83	20.75	21.03	20.76	20.43	21.58	19.09
ZPVE (B3LYP)	20.75	20.54	20.24	21.67	21.86	21.12	21.09	21.63	19.59

[a] Zero-point vibrational energy differences were obtained at the MP2=full/6-31G* level (MP2, MP4, and PMP4) or at the B3LYP/6-311G** level (B3LYP and QCISD(T)).

$SiC_3H_2^+(^2B_1)$:

$$\{core\}\ 7a_1^2\ 8a_1^2\ 9a_1^2\ 10a_1^2\ 2b_2^2\ 2b_1^2\ 11a_1^2\ 3b_2^2\ 3b_1^1$$

$SiC_3H_2^+(^2B_2)$:

$$\{core\}\ 7a_1^2\ 8a_1^2\ 9a_1^2\ 10a_1^2\ 2b_2^2\ 2b_1^2\ 11a_1^2\ 3b_2^2\ 4b_2^1$$

It is readily seen that both electronic configurations correlate with $Si^+ + l\text{-}C_3H_2$. Vinylidenecarbene has the following electronic configuration

$l\text{-}C_3H_2$

$$(^1A_1):\ 1a_1^2\ 2a_1^2\ 3a_1^2\ 4a_1^2\ 5a_1^2\ 6a_1^2\ 1b_2^2\ 7a_1^2\ 1b_1^2\ 2b_2^2$$

whereas $Si^+(^2P)$, under C_{2v} symmetry, splits into three spatially degenerate states

$$Si^+(^2P,^2B_1):\ 1a_1^2\ 2a_1^2\ 3a_1^2\ 1b_2^2\ 1b_1^2\ 4a_1^2\ 2b_1^1$$

$$Si^+(^2P,^2B_2):\ 1a_1^2\ 2a_1^2\ 3a_1^2\ 1b_2^2\ 1b_1^2\ 4a_1^2\ 2b_2^1$$

$$Si^+(^2P,^2A_1):\ 1a_1^2\ 2a_1^2\ 3a_1^2\ 1b_2^2\ 1b_1^2\ 4a_1^2\ 2a_1^1$$

The $^2B_1$ and $^2B_2$ states correspond to the structures **15** and **16**. We have also searched for the $^2A_1$ state, but our attempts led to a different electronic configuration of the same symmetry

$SiC_3H_2^+(^2A_1)$:

$$\{core\}\ 7a_1^2\ 8a_1^2\ 9a_1^2\ 10a_1^2\ 2b_2^2\ 2b_1^2\ 3b_2^2\ 3b_1^2\ 11a_1^1$$

which does not correlate with $Si^+(^2P,^2A_1) + l\text{-}C_3H_2(^1A_1)$. Since this $^2A_1$ state was found to lie much higher in energy than the other two states, and has an imaginary frequency at both MP2 and B3LYP levels, it will not be discussed further. The fact that the $^2B_1$ and $^2B_2$ states are favored over the $^2A_1$ one is not surprising. The interaction of Si^+ with $l\text{-}C_3H_2$ through the end carbon along the $^2B_2$ or $^2B_1$ surfaces is clearly attractive, since there is a possibility for donation of electron density from the lone pair of carbon toward the vacant p_z orbital (a_1 symmetry) of silicon. On the other hand, the $^2A_1$ surface should be less favorable since in that case there is an electron occupying the $3p_z$ orbital and therefore we have a three-electron interaction.

Of the two states, $^2B_1$ and $^2B_2$, the former is much more stable, since there is also a favorable π-interaction between the $2b_2$ orbital of vinylidenecarbene and the vacant p orbital of the same symmetry. In the case of the $^2B_2$ state the unpaired electron occupies that p orbital and therefore there is an unfavorable three-electron interaction. This results in a much longer Si−C distance for the $^2B_2$ state than for the $^2B_1$ one. On the other hand, the rest of geometrical parameters are very similar for both states.

Another open-chain structure (**17**) has also been characterized, corresponding to a $^2A'$ electronic state. The $^2A''$ state is only obtained at the Hartree−Fock level, whereas at both the MP2 and B3LYP levels it collapses into the cyclic structure **18**. In the case of structure **17** there is a hydrogen atom bonded to the central carbon atom. Both carbon−carbon bond distances are quite similar and close to typical double bond lengths. As can be seen in Table 4, this is the less stable of all $(SiC_3H_2)^+$ structures presented in this work.

Structures **18** and **19** result from the interaction of Si^+ with cyclopropenylidene through an apex, a carbon atom which has a lone pair. The corresponding electronic configurations for these structures, which have $^2B_1$ and $^2B_2$ electronic states respectively, are the following:

$SiC_3H_2^+(^2B_1)$:

$$\{core\}\ 6a_1^2\ 3b_2^2\ 7a_1^2\ 8a_1^2\ 9a_1^2\ 2b_1^2\ 4b_2^2\ 10a_1^2\ 3b_1^1$$

$SiC_3H_2^+(^2B_2)$:

$$\{core\}\ 6a_1^2\ 3b_2^2\ 7a_1^2\ 8a_1^2\ 9a_1^2\ 2b_1^2\ 4b_2^2\ 10a_1^2\ 5b_2^1$$

Both states correlate with $Si^+(^2P) + c\text{-}C_3H_2(^1A_1)$, since cyclopropenylidene has the following ground-state configuration:

$c\text{-}C_3H_2(^1A_1)$:

$$1a_1^2\ 2a_1^2\ 1b_2^2\ 3a_1^2\ 2b_2^2\ 4a_1^2\ 5a_1^2\ 3b_2^2\ 1b_1^2\ 6a_1^2$$

On the other hand the lowest-lying $^2A_1$ state corresponds to the following electronic configuration

$SiC_3H_2^+(^2A_1)$:

$$\{core\}\ 6a_1^2\ 7a_1^2\ 3b_2^2\ 8a_1^2\ 9a_1^2\ 2b_1^2\ 4b_2^2\ 3b_1^2\ 10a_1^1$$

and therefore does not correlate with $Si^+(^2P,^2A_1) + c\text{-}C_3H_2(^1A_1)$. Since this state lies much higher in energy than the other two three-membered ring structures (about 77 kcal/mol at the B3LYP level), it will not be considered further. The reason for the higher stability of the $^2B_1$ and $^2B_2$ states compared with the $^2A_1$ one is the same as in the case of the structures derived from $l\text{-}C_3H_2$. In the case of $^2B_1$ and $^2B_2$ states there is a favorable interaction between the lone pair of the carbon and the vacant p_z (a_1 symmetry) orbital of Si^+. The $^2B_1$ state is favored over the $^2B_2$ state in this case due to an additional delocalization of the b_1 electron of $Si^+(^2P,^2B_1)$ into the b_1 orbital of the carbon atom (although in $c\text{-}C_3H_2$ the $1b_1$ orbital is formally delocalized over the entire molecule, it is essentially located between the two symmetric carbon atoms). This results in a much shorter Si−C bond distance for the $^2B_1$ state, as can be seen in Figure 2.

The rest of the $(SiC_3H_2)^+$ structures shown in Figure 2 are four-membered rings. Structure **20** can be viewed as the result of the interaction of Si^+ with a side of c-C_3H_2, whereas structures **21** and **22** are obtained from **20** through migration of a hydrogen atom to a carbon atom, and structure **23** from migration of a hydrogen atom to silicon. The main difference between MP2 and B3LYP geometries for these species concern structure **22**, which is found to be asymmetric at the MP2 level, but has a symmetric structure ($^2A_1$ electronic state) at the B3LYP level. As can be seen in Figure 2, in structures **20** and **21** there are no transannular C−C bondings since at least one (**20**) or both (**21**) carbon atoms are bonded to hydrogen atoms. This results in a long C_1-C_3 distance in both cases. On the other hand, a very short transannular C_1-C_3 bond distance (1.408 Å) is found for **22** and even in structure **23** the bond distance (1.552 Å at the B3LYP level) suggests the possibility of transannular C−C bonding.

The energy results shown in Table 4 show that **20**, which is the direct result of the interaction of Si^+ with c-C_3H_2, is the most stable four-membered ring structure, followed by **21** which has also two C−H bonds. It is also noticeable that migration of a hydrogen atom to a silicon atom (**23**) results in a more stable structure than migration to a carbon already bonded to a hydrogen atom (**22**).

The most important conclusion from the relative energy values shown in Table 4 is that the two most stable $(SiC_3H_2)^+$ species are, by far, those obtained from the bonding of Si^+ with l-C_3H_2 and c-C_3H_2 through an electron lone-pair (structures **15** and **18**).

It is worth pointing out that attachment of the silicon cation changes the stability order of the open-chain and three-membered ring structures. Cyclopropenylidene is more stable than vinylidenecarbene by more than 10 kcal/mol (12.5, 11.1, and 11.8 at the PMP4, B3LYP, and QCISD(T), respectively). On the other hand, the open-chain structure **15** lies below the cyclic isomer **18** by more than 8 kcal/mol at the PMP4 and QCISD(T) levels, and by 12 kcal/mol at the B3LYP level. Since in both cases the bonding is of a dative nature (interaction of Si^+ with a vacant p_z orbital with a lone pair), one should expect in principle that the stability order could remain. However, there is an additional interaction which contributes to the bonding. Whereas in the case of **15** there is a delocalization of two $2b_2$ electrons of l-C_3H_2 into a second vacant 3p orbital of Si^+, for structure **18** only delocalization of one b_1 electron of Si^+ into the vacant carbon orbital of the same symmetry contributes to the bonding. In fact, the Si−C bond distance is much shorter in **15** than in structure **18**. The stability order for $(SiC_3H_2)^+$ isomers is in contrast with that found for the triplet $(PC_3H_2)^+$ species.[28] In the case of the $(PC_3H_2)^+$ system, the cyclic isomer resulting from the interaction of phosphorus ion with c-C_3H_2 is lower in energy (about 8.6 kcal/mol at the PMP4 level) than the open-chain isomer obtained from the attachment of P^+ to the end carbon of l-C_3H_2. P^+ ions (^3P ground state) can only form a dative bond with either c-C_3H_2 or l-C_3H_2 through the carbon lone pair. Therefore, the relative energy is very close to that found for the two hydrocarbons.

From the values of Table 4 it is clear that the most obvious targets for a possible experimental detection are structures **15** and **18**. The IR spectrum of **15** should be dominated by symmetric C−C stretching which is predicted to be the most intense at both MP2 and B3LYP levels, and its fundamental is estimated at 2113 cm^{-1} (unscaled MP2) and 1979 cm^{-1} (B3LYP). In the case of **18** the most intense band corresponds to a symmetric stretching of the C_3 unit at 1231 cm^{-1} (MP2) or 1216 cm^{-1} (B3LYP).

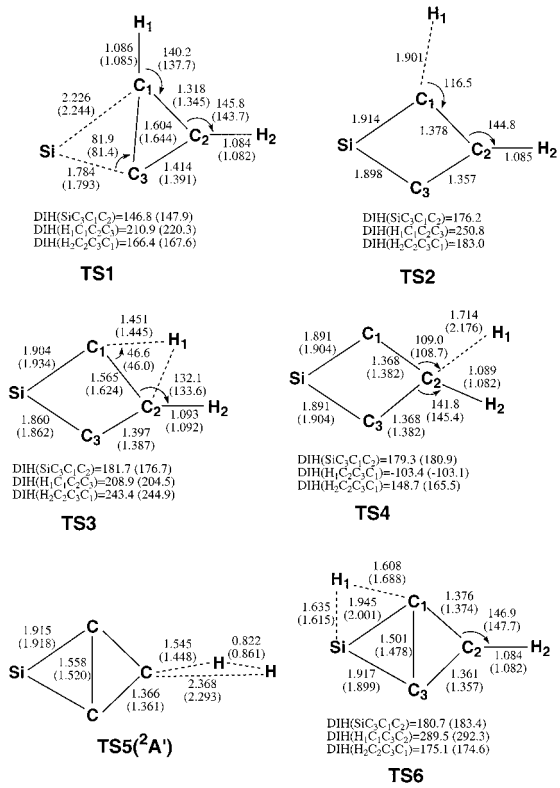

Figure 3. MP2/6-31G* and B3LYP/6-311G** (in parentheses) optimized geometries for the relevant transition states involved in the reaction of Si^+ with c-C_3H_2. Distances are given in angstroms and angles in degrees.

Reaction of Si^+ with C_3H_2. In this section we will discuss the reaction of silicon ions with either cyclopropenylidene or vinylidenecarbene. Basically, there are in principle three different channels for this reaction: production of SiC_3H^+, production of SiC_3^+, and charge transfer

$$\rightarrow SiC_3H^+ + H(^2S)$$

$$Si^+(^2P) + C_3H_2(^1A_1) \rightarrow SiC_3^+ + H_2(^1\Sigma_g^+)$$

$$\rightarrow Si(^3P) + C_3H_2^+(^2A_1)$$

The possible SiC_3H^+ structures have already been discussed, whereas the different SiC_3^+ isomers have been considered in a previous work.[17] Charge transfer can be discarded because of its endothermicity since silicon has a lower ionization potential (7.8 eV at the PMP4 level) than both cyclopropenylidene and vinylidenecarbene (8.6 and 10.3 eV, respectively, at the PMP4 level). Other possibilities, such as the abstraction channels leading to either $SiH^+ + C_3H$ or $SIH + C_3H^+$, have also been considered. However, these channels were also found to be clearly endothermic (see Tables 5 and 6).

First, we will present the results for the reaction of Si^+ with c-C_3H_2. The relative energies (with respect to the reactants) of the possible products, intermediates, and relevant transition states are given in Table 5 at different levels of theory. In Figure 3, the geometries of the transition states are shown, whereas the energy profile for the reaction of $Si^+ + $ c-C_3H_2 at selected levels of theory (PMP4 and QCISD(T)) is shown in Figure 4.

As can be seen in Table 5 there is a very good agreement in this case at all levels of theory. In fact, the PMP4 and QCISD-

TABLE 5: Relative Energies (kcal/mol) at Different Levels of Theory with the 6-311G Basis Set of the Species Involved in the Reaction of Si^+ with c-C_3H_2[a]**

						ΔZPVE	
	MP2	MP4	PMP4	B3LYP	QCISD(T)	MP2	B3LYP
			Reactants				
Si^+ + c-C_3H_2	0.0	0.0	0.0	0.0	0.0		
			Intermediates				
18($^2B_1$)	−89.9	−88.3	−88.5	−95.4	−88.6	1.36	1.53
19($^2B_2$)	−74.0	−72.5	−72.8	−76.5	−72.3	1.65	1.72
20(^2A)	−66.6	−66.8	−69.6	−71.5	−69.8	1.38	0.98
21($^2A'$)	−60.0	−60.2	−63.4	−67.0	−63.8	1.05	0.95
22(^2A)	−48.0	−47.9	−49.7	−47.4	−48.4	2.20	1.49
23($^2A'$)	−58.4	−54.1	−54.2	42.4	−52.0	−0.29	−0.55
			Transition States				
TS1	−61.7	−61.4	−64.4	−68.7	−65.5	0.56	0.15
TS2	−13.5	−11.0	−13.5	-	-	−4.23	-
TS3	−20.7	−19.4	−21.3	−21.6	−19.9	−1.12	−1.95
TS4	−10.7	−8.2	−9.3	−7.7	−8.3	−3.60	−4.86
TS5	5.2	5.4	3.6	1.5	5.7	−5.89	−6.77
TS6	−22.8	−21.8	−25.5	−26.5	−23.2	−2.26	−2.65
			Products				
SiC_3H^+ (**7**) + H	−18.4	−14.4	−14.4	−8.2	−11.9	−5.37	−5.57
SiC_3H^+ (**11**) + H	7.6	7.1	7.1	10.6	8.6	−6.06	−6.39
SiC_3^+ ($^2A_1$) + H_2	−1.7	−2.0	−2.8	−0.2	−1.9	−6.14	−6.60
SiC_3^+ ($^2B_2$) + H_2	22.7	15.1	11.0	12.8	11.5	−6.55	−7.45
SiH^+ + c-C_3H($^2B_2$)	30.4	28.3	27.5	26.9	28.3	5.54	5.11
SiH + c-C_3H^+($^1A_1$)	80.8	77.2	77.1	79.2	74.6	4.19	5.47

[a] Zero-point vibrational energy differences were obtained at the MP2=full/6-31G* level (MP2, MP4, PMP4) or at the B3LYP/6-311G** level (B3LYP and QCISD(T)). The imaginary frequencies for the transition states at the MP2=full/6-31G* level (B3LYP/6-311G** values in parentheses) are the following: TS1: 719i (495i); TS2; 1115i; TS3: 1205i (1176i); TS4: 1174i (346i); TS5: 1182i (644i); TS6: 1431i (1039i).

TABLE 6: Relative Energies (kcal/mol) at Different Levels of Theory with the 6-311G Basis Set of the Species Involved in the Reaction of Si^+ with l-C_3H_2[a]**

						ΔZPVE	
	MP2	MP4	PMP4	B3LYP	QCISD(T)	MP2	B3LYP
			Reactants				
Si^+ + l-C_3H_2	0.0	0.0	0.0	0.0			
			Intermediates				
15($^2B_1$)	−106.8	−103.7	−109.6	−118.4	−109.2	1.96	1.37
16($^2B_2$)	−59.1	−56.5	−62.7	−73.0	−66.2	1.71	1.16
17($^2A'$)	−26.9	−26.0	−32.8	−43.9	−38.0	2.20	0.86
			Transition States				
TS7($^2A''$)	−14.8	−11.6	−24.1	−27.1	−19.3	−4.88	−5.47
TS8($^2A'$)	22.3	22.4	9.2	−7.3	−0.3	1.03	−5.06
TS9($^2A''$,^2A)	−24.5	−23.8	−28.6	−51.3	−39.9	0.89	−2.09
TS10($^2A'$)				−1.4	9.8		−3.00
TS11($^2A'$)	22.9	22.8	10.3	−1.4	6.7	−4.07	−4.92
TS12(s.o.s.p)				56.6	69.2		−6.16
			Products				
$SiCCCH^+$($^1\Delta$) + H	−8.9	−5.2	−5.2	−8.0	−3.3	−6.23	−5.43
$SiCCCH^+$($^3\Sigma$) + H	−15.7	−12.5	−19.7	−26.9	−19.5	−6.03	−5.63
SiC_3^+($^2\Pi$) + H_2	10.2	6.8	0.8	−10.3	−6.8	−5.60	−6.42
SiH^+ + l-C_3H($^2\Pi$)	30.0	27.7	22.2	15.4	17.1	2.95	3.93
SiH + l-C_3H^+($^2\Sigma$)	45.1	41.8	41.7	45.1	44.3	2.99	4.07

[a] Zero-point vibrational energy differences were obtained at the MP2=full/6-31G* level (MP2, MP4, PMP4) or at the B3LYP/6-311G** level (B3LYP and QCISD(T)). The imaginary frequencies for the transition states at the MP2=full/6-31G* level (B3LYP/6-311G** values in parentheses) are the following: TS7: 186i (58i); TS8; 1222i (349i); TS9: 591i (798i); TS10: (2029i); TS11: 1449i (882i); TS12: (1301i).

(T) results are within 2 kcal/mol in most cases. It is also interesting to point out that B3LYP values are very close to the most realiable ab initio values (the worst case being the relative energy of **19**). The most important discrepancy is found for TS2, since this transition state is not found at the B3LYP level (our attempts to optimize this transition state at the B3LYP level led to TS6).

It is readily seen in Table 5 that production of SiC_3H^+ is exothermic only in the case of the most stable isomer, structure **7** corresponding to C_{2v} symmetry. Production of isomer **11** (C_s symmetry) is clearly endothermic at all levels of theory. The channel leading to SiC_3^+ is also slightly exothermic only for its cyclic $^2A_1$ ground state. Formation of the other low-lying four-membered ring ($^2B_2$ electronic state[17]) is endothermic by more than 11 kcal/mol. Therefore, we will only consider the reaction channels for the production of the ground states of SiC_3H^+ and SiC_3^+.

The first step for all channels should be attachment of Si^+ to c-C_3H_2, leading to either the $^2B_1$ or $^2B_2$ states, the former being the preferred one. Both species may isomerize into the four-

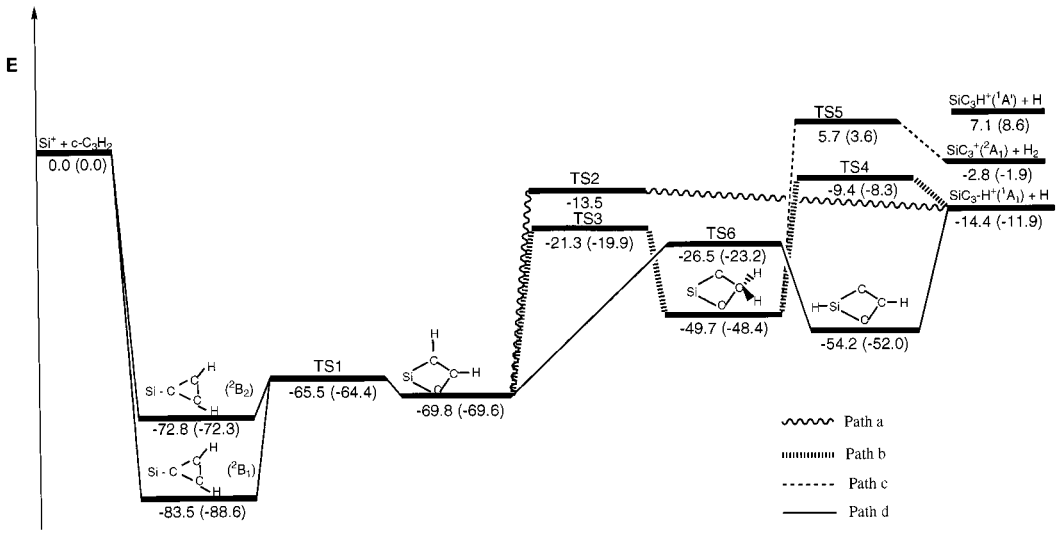

Figure 4. Energy profile, in kcal/mol, for the reaction of Si^+ with c-C_3H_2 at the PMP4 and QCISD(T) (in parentheses) levels. ΔZPVE corrections have been included at the MP2/6-31G* and B3LYP/6-311G** levels, respectively.

membered ring **20**, following a nonsymmetric path which involves transition state TS1

$$Si^+ + c\text{-}C_3H_2 \rightarrow SiC_3H_2^+ (\mathbf{18}, \mathbf{19}) \xrightarrow{TS1} SiC_3H_2^+ (\mathbf{20})$$

TS1 lies well below the reactants (about 65 kcal/mol at both PMP4 and QCISD(T) levels), and therefore formation of **20** is easily obtained. All feasible mechanisms start now from this species. One possibility is direct hydrogen elimination from **20** leading to SiC_3H^+

$$SiC_3H_2^+ (\mathbf{20}) \xrightarrow{TS2} SiC_3H^+ (\mathbf{7}) + H \qquad (a)$$

The implied transition state, TS2, is also nonplanar and is found to lie about 13.5 kcal/mol below reactants at the PMP4 level. This transition state is not obtained at the B3LYP level, suggesting that hydrogen atom loss at this level of theory takes place directly without any barrier (only the difference in stability between **20** and $SiC_3H^+ + H$). In fact, the relative energies of TS2 at the PMP4 level (−13.5) is very close to the value for the products (−14.4), suggesting that maybe at higher levels of theory this transition state could disappear. In any case, since TS2 lies below $Si^+ + c\text{-}C_3H_2$, path (a) is feasible under intrestellar conditions.

Another possibility is isomerization of **20** into **22**, the isomer with two hydrogens bonded to the same carbon atom. This species may undergo hydrogen atom elimination or hydrogen molecule abstraction leading, respectively, to $SiC_3H^+ + H$ or $SiC_3^+ + H_2$.

$$SiC_3H_2^+ (\mathbf{20}) \xrightarrow{TS3} SiC_3H_2^+ (\mathbf{22}) \xrightarrow{TS4} SiC_3H^+ (\mathbf{7}) + H \quad (b)$$

$$SiC_3H_2^+ (\mathbf{20}) \xrightarrow{TS3} SiC_3H_2^+ (\mathbf{22}) \xrightarrow{TS5} SiC_3^+ (^2A_1) + H_2 \quad (c)$$

Whereas both TS3 and TS4 are found to lie below the reactants at all levels of theory, and consequently path (b) may take place, TS5 is slightly higher in energy than $Si^+ + c\text{-}C_3H_2$. Therefore, path (c) implies a small barrier which could hinder production of cyclic SiC_3^+ through this mechanism, or at least favor the other channel leading to SiC_3H^+. We should point out that all our attempts to obtain an optimized structure for TS5 with two equivalent C−H bond distances failed, since a second-order saddle point was always obtained. Allowing different C−H bond distances led to the structure shown in Figure 3, in which the hydrogen atoms are in a quasi-linear arrangement.

Finally, there is another path starting from **20** which involves isomerization into **23** through migration of a hydrogen atom to silicon, followed by elimination of hydrogen:

$$SiC_3H_2^+ (\mathbf{20}) \xrightarrow{TS6} SiC_3H_2^+ (\mathbf{23}) \rightarrow SiC_3H^+ (\mathbf{7}) + H \qquad (d)$$

Only elimination of the hydrogen atom bonded to silicon may lead to exothermic products. Path (d) is also feasible since the first step implies transition state TS6, which is well below the reactants at all levels of theory, whereas elimination of hydrogen from silicon takes place directly without any barrier (we have carried out a scan for this process, performing optimizations at different Si−H distances, and found no sign of a transition state).

We may conclude that for the reaction of Si^+ with cyclopropenylidene there are three different mechanisms which lead to cyclic SiC_3H^+, paths (a), (b), and (d), which are barrier-free. Furthermore, charge transfer is not a competitive process, since it is endothermic. On the other hand, production of SiC_3^+ is slighly exothermic but involves a small barrier. Therefore, the preferred channel is production of SiC_3H^+.

The results for the reaction of Si^+ with vinylidenecarbene are shown in Table 6. The geometries of the transition states involved in this case are given in Figure 5, and the energy profile for the reaction at the PMP4 and QCISD(T) levels is shown in Figure 6.

Inspection of the results given in Table 6 shows that there are significant differences between QCISD(T) and PMP4 values in this case. The discrepancy is even higher between PMP4 and B3LYP values, with differences up to 22 kcal/mol (TS9), and reversed signs in the relative energies (TS8, TS1, $SiCCC^+ + H_2$). Furthermore, there are two transition states, namely TS10 and TS12, which could be obtained only at the B3LYP level, since our attempts at the MP2 level failed. The discrepancy between DFT and MP results can be partly ascribed to the spin contamination, which is very high for the HF wavefunctions of some of the intermediates and transition states for this reaction, whereas it is virtually negligible when density functional theory is employed. Therefore, since spin contamination may severely affect the convergence of the MP series, the B3LYP results should be more reliable. For the reaction of Si^+ with the cyclic

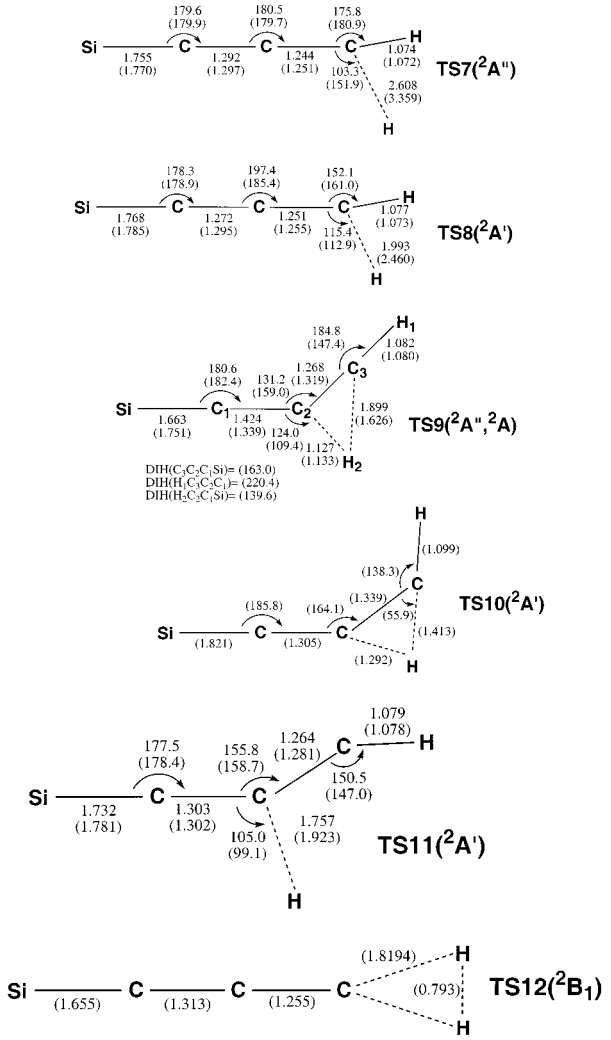

Figure 5. MP2/6-31G* and B3LYP/6-311G** (in parentheses) optimized geometries for the relevant transition states involved in the reaction of Si^+ with l-C_3H_2. Distances are given in angstroms and angles in degrees.

hydrocarbon, spin contamination of the HF wave functions was much lower and in many cases virtually negligible too. We have seen in that case a good agreement between DFT and ab initio methods.

According to the B3LYP and QCISD(T) results shown in Table 6, production of the singlet and triplet states of $SiCCCH^+$, as well as production of $SiCCC^+ + H_2$, are all exothermic channels. On the other hand, MP4 theory predicts an endothermicity of 6.8 kcal/mol for the last of these processes, which is further reduced upon projection to near thermoneutrality (0.8 kcal/mol at the PMP4 level).

The first step in the reaction is the attachment of Si^+ to $:CCCH_2$ through a dative bond. Two species, **15** ($^2B_1$) and **16** ($^2B_2$), can be formed. The $^2B_1$ state is clearly favored because of its higher stability. Once these species are formed, hydrogen atom elimination may occur leading directly to triplet $SiCCCH^+$ in the case of the $^2B_1$ state, and to singlet $SiCCCH^+$ when the reaction proceeds through the $^2B_2$ state:

$$Si^+ + \text{l-}C_3H_2 \rightarrow SiCCCH_2^+(^2B_1) \xrightarrow{TS7} SiCCCH^+(^3\Sigma) + H \quad \text{(e)}$$

$$Si^+ + \text{l-}C_3H_2 \rightarrow SiCCCH_2^+(^2B_2) \xrightarrow{TS8} SiCCCH^+(^1\Delta) + H \quad \text{(f)}$$

We have characterized both transition states, TS7 and TS8, which are of $^2A''$ and $^2A'$ symmetry, respectively. In both cases, the C−H distance of the broken bond is relatively large, especially for the $^2A''$ state, and the rest of geometrical parameters are very close to those of the respective final products. Whereas TS7 is clearly predicted to lie below the reactants at all levels of theory, very different results are obtained for TS8 depending on the theoretical method employed. MP2 and MP4 levels place this transition state more than 20 kcal/mol above $Si^+ + \text{l-}C_3H_2$, an energy difference which is substantially reduced at the projected-MP4 level. On the other hand, B3LYP predicts that TS8 should lie below the reactants, and QCISD(T) provides a value of just −0.3 kcal/mol. In any case, it is clear that, even if it is quite likely that path (f) is finally barrier-free, path (e) should be not only thermochemically but also kinetically favored over path (f).

In addition, there are other possible paths for the reaction. Isomerization of structures **15** and **16** may occur. In the case of **15**($^2B_1$) migration of a hydrogen atom proceeds through transition state TS9 (which is nonplanar at the B3LYP level) and leads directly to the cyclic isomer **18**($^2B_1$), since there is no a stable open-chain structure similar to **17**, corresponding to $^2A''$ electronic state. Therefore, this path (g) leads to structure **18**:

$$Si^+ + \text{l-}C_3H_2 \rightarrow SiCCCH_2^+(^2B_1) \xrightarrow{TS9} SiC_3H_2^+ \ (\mathbf{18}) \quad \text{(g)}$$

This path connects the reaction initiated with the open-chain hydrocarbon with a cyclic structure which may undergo the same processes considered when the reaction started with c-C_3H_2. Therefore, it may finally lead to the cyclic SiC_3H^+ isomer **7**.

Migration of a hydrogen atom in structure **16**($^2B_2$) leads to the isomer **17**, which has a $^2A''$ electronic state. We were able to characterize the corresponding transition state, TS10, at the B3LYP level. At the MP2 level we obtained a second-order saddle point (two imaginary frequencies, one of them corresponding to out-of-plane bending), and all our attempts to optimize this transition state without symmetry failed. Therefore, only the B3LYP geometry, as well as B3LYP and QCISD(T) realtive energies, are provided in this case. Once structure **17** is formed, hydrogen atom elimination could lead to the final product, singlet $SiCCCH^+$, through transition state TS11. This path, (h), can be summarized as follows

$$Si^+ + \text{l-}C_3H_2 \rightarrow SiCCCH_2^+(^2B_2) \xrightarrow{TS10} SiCCHCH^+(^2A') \xrightarrow{TS11} SiCCCH^+(^1\Delta) + H \quad \text{(h)}$$

Both transition states, TS10 and TS11, are predicted to lie slightly below the reactants, at the B3LYP level. However, at the QCISD(T) level both lie above the reactants by 9.8 and 6.7 kcal/mol, respectively. The PMP4 value for TS11 predicts an even higher barrier of 10.3 kcal/mol. Then it is quite likely that, considering the QCISD(T) values as the most reliable ones, path (h) could be affected by a nonnegligible barrier.

Finally, we have also considered elimination of a hydrogen molecule from $SiCCCH_2^+$. We were only able to obtain at the B3LYP level a C_{2v}-symmetric structure for the corresponding transition state TS12, when the reaction starts from the $SiCCCH_2^+$ $^2B_1$ state (structure **15**). In fact, TS12 is a second-order saddle point, since it has two imaginary frequencies. One of the associated modes corresponds to elimination of H_2, whereas the second one is of b_2 symmetry and points to distortion of the C_{2v} symmetry with two different C−H distances and CCH angles. Our attempts to obtain this transition state in C_s

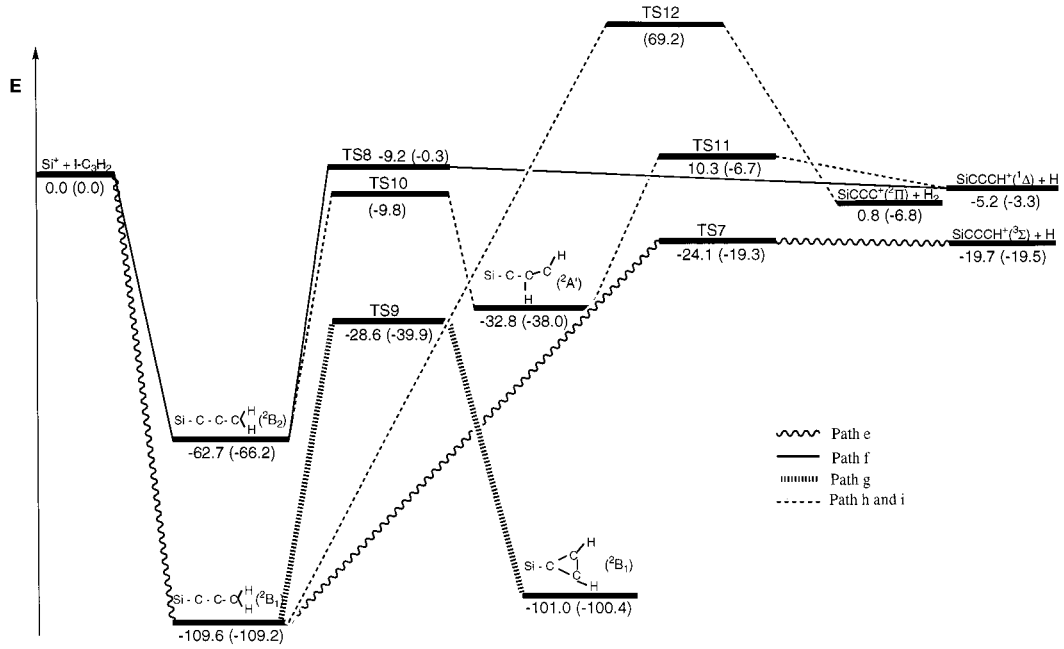

Figure 6. Energy profile, in kcal/mol, for the reaction of Si^+ with l-C_3H_2 at the PMP4 and QCISD(T) (in parentheses) levels. ΔZPVE corrections have been included at the MP2/6-31G* and B3LYP/6-311G** levels, respectively.

symmetry (following the second mode with imaginary frequency) led to transition state TS7. In the case of the $^2B_2$ state (structure **16**) we were unable to obtain even a second-order saddle point.We have reported the relative energies at the B3LYP and QCISD(T) level of TS12 (in fact a second-order saddle point) in order to have at least a crude estimate of the possible barrier associated to this process

$$Si^+ + l\text{-}C_3H_2 \rightarrow SiCCCH_2^+(^2B_1) \xrightarrow{TS12} SiCCC^+(^2\Pi) + H_2 \quad \text{(i)}$$

Both levels predict that TS12 should lie high above the reactants (56.6 and 69.2 kcal/mol at the B3LYP and QCISD(T) levels, respectively). Therefore, the barrier associated to path (i) seems high enough to discard the feasibility of this channel, even if our results are based on an approximation. It is also expected that the activation barrier should be of the same magnitude when structure **16**($^2B_2$) is initially formed.

Conclusions

A theoretical study of the $(SiC_3H)^+$ and $(SiC_3H_2)^+$ species has been carried out at two different levels of theory. Geometries and vibrational frequencies for the different isomers have been obtained at the MP2/6-31G* and B3LYP/6-311G** levels. Electronic energies have been computed at the MP4/6-311G**//MP2/6-31G* and QCISD/T)/6-311G**//B3LYP/6-311G** levels. All theoretical levels, except B3LYP, predict that the global minimum of the $(SiC_3H)^+$ system is a cyclic isomer (structure **7**), with $^1A_1$ electronic state, which is derived from protonation of the SiC_3 ground state. On the other hand, a linear triplet state (structure **2**) is predicted to lie more than 7 kcal/mol below structure **7** at the B3LYP level. Since a good correlated level is usually required for analyzing the competition between cyclic and noncyclic structures, the ab initio results seem more reliable than DFT ones in this case, and therefore structure **7** seems the most likely candidate to the $(SiC_3H)^+$ ground state.

The proton affinities of the three lowest-lying isomers of SiC_3 have been computed. A good agreement between the PA's at different levels of theory is obtained. The three isomers have relatively high proton affinities (about 230 kcal/mol for the cyclic ground state, 228 kcal/mol for the linear isomer, and 215 kcal/mol for the four-membered ring with transannular Si−C bonding). This means that SiC_3 species should be easily protonated in interstellar media.

The two most stable $(SiC_3H_2)^+$ species are those formally obtained from the bonding of Si^+ with vinylidenecarbene and cyclopropenylidene through an electron lone pair, resulting in structures **15** and **18**, respectively. Nevertheless, the attachment of the silicon cation results in a reversed stability order, since **15** (derived from l-C_3H_2) is predicted to lie below **18** (obtained from c-C_3H_2) by 9 kcal/mol (PMP4 and QCISD(T)) or 12 kcal/mol (B3LYP).

In the case of the reaction of Si^+ with c-C_3H_2 charge transfer is not a competitive process because of its endothermicity. On the other hand, production of SiC_3^+ is only slightly exothermic (around −2 kcal/mol), whereas production of cyclic SiC_3H^+ (**7**) is clearly exothermic (more than 10 kcal/mol at the most realiable levels of theory). Production of SiC_3^+ is subject to a small energy barrier (ranging from 1.5 to 5.7 kcal/mol depending on the level of theory employed), whereas there are three different mechanisms leading to cyclic SiC_3H^+ which are barrier-free. Therefore, the most favorable channel for this reaction is production of cyclic SiC_3H^+.

For the reaction of Si^+ with l-C_3H_2 charge transfer is also endothermic, whereas production of linear $SiCCC^+$ and singlet and triplet linear $SiCCCH^+$ is all exothermic. Five different mechanisms have been explored. One of these paths connects with a cyclic structure which finally could lead to the cyclic SiC_3H^+ isomer. This seems the preferred channel for this reaction, since it takes place through a transition state which lies well below those involved in the other paths. Only production of the triplet linear isomer, through direct hydrogen elimination from the lowest-lying $SiC_3H_2^+$ isomer **15**, seems to be competitive. Production of $SiCCC^+$ seems to proceed through a significant barrier, whereas the singlet linear isomer involves small energy barriers.

Therefore, the main conclusion of the present work is that the reactions of Si^+ with c-C_3H_2 and l-C_3H_2 are feasible in the

interstellar medium, and the preferred product should be cyclic SiC_3H^+. Only production of the linear $SiCCCH^+$ isomer (in its triplet ground state) seems to be competitive. Therefore, these reactions could be possible sources of SiC_3 in space. In addition, from the comparison of B3LYP and ab initio results, it is observed that both theoretical methods are generally in relative good agreement when spin contamination is not too high, except in those cases where correlation effects are very important. On the other hand, when spin contamination is significant (for example in some of the intermediates and transition states involved in the reaction of Si^+ with l-C_3H_2), important differences between DFT and ab initio results are found.

Acknowledgment. This research has been supported by the Ministerio de Educación y Cultura of Spain (DGICYT, Grant PB97-0399-C03-01) and by the Junta de Castilla y León (Grant VA 21/97).

Supporting Information Available: Tables of vibrational frequencies and IR intensities for the different $(SiC_3H_2)^+$ isomers. This material is available free of charge via the Internet at http://pubs.acs.org. See any current masthead page for ordering information.

References and Notes

(1) Parsons, J. D.; Bunshah, R. F.; Stafsudd, O. M. *Solid State Technol.* **1985**, *28*, 133.

(2) Cernicharo, J.; Gottlieb, C. A.; Guelin, M.; Thaddeus, P.; Vrtilek, J. M. *Astrophys. J. Lett.* **1989**, *341*, L25.

(3) Thaddeus, P.; Cummins, S. E.; Linke, R. A. *Astrophys. J. Lett.* **1984**, *283*, L25.

(4) Ohishi, M.; Kaifu, N.; Kawaguchi, K.; Murakami, A.; Saito, S.; Yamamoto, S.; Ishikawa, S.; Fujita, Y.; Shiratori, Y.; Irvine, W. M. *Astrophys. J. Lett.* **1989**, *345*, L83.

(5) Saito, S.; Kawaguchi, K.; Yamamoto, S.; Ohishi, M.; Suzuki, H.; Kaifu, N. *Astrophys. J.* **1987**, 317, L115.

(6) Yamamoto, S.; Saito, S.; Kawaguchi, K.; Kaifu, N.; Suzuki, H.; Ohishi, M. *Astrophys. J.* **1987**, 317, L119.

(7) Alberts, I. L.; Grev, R. S.; Schaefer, H. F. *J. Chem. Phys.* **1990**, *93*, 5046.

(8) Herbst, E.; Millar, T. J.; Wlodek, S.; Bohme, D. K. *Astron. Astrophys.* **1989**, 222, 205.

(9) Creasy, W. R.; O'Keefe, A.; McDonald, J. R. *J. Phys. Chem.* **1987**, *91*, 2848.

(10) Wlodek, S.; Fox, A.; Bohme, D. K. *J. Am. Chem. Soc.* **1991**, *113*, 4461.

(11) Largo, A.; Barrientos, C. *J. Phys. Chem.* **1994**, *98*, 3978.

(12) Thaddeus, P.; Vrtilek, J. M.; Gottlieb, C. A. *Astrophys. J.* **1985**, 299, L63.

(13) Cernicharo J.; Gottlieb, C. A.; Guelin, M.; Killian, T. C.; Paubert, G.; Thaddeus, P.; Vrtilek, J. M. *Astrophys. J.* **1991**, 368, L39.

(14) DeFrees, D. J.; McLean, A. D. *Astrophys. J.* **1986**, 308, L31.

(15) Jonas, V.; Bohme, M.; Frenking, G. *J. Phys. Chem.* **1992**, *96*, 1640.

(16) del Río, E.; Barrientos, C.; Largo, A. *J. Phys. Chem.* **1996**, *100*, 14643.

(17) Redondo, P.; Sagüillo, A.; Largo, A. *J. Phys. Chem.* **1998**, *102*, 3953.

(18) Francl, M. M.; Pietro, W. J.; Hehre, W. J.; Binkley, J. S.; Gordon, M. S.; DeFrees, D. J.; Pople, J. A. *J. Chem. Phys.* **1982**, *77*, 3654.

(19) Becke, A. D. *J. Chem. Phys.* **1993**, *98*, 5648.

(20) Krishnan, R.; Binkley, J. S.; Seeger, R.; Pople, J. A. *J. Chem. Phys.* **1980**, *72*, 650.

(21) McLean, A. D.; Chandler, G. S. *J. Chem. Phys.* **1980**, *72*, 5639.

(22) Pople, J. A.; Krishnan, R. *Int. J. Quantum Chem.* **1978**, *14*, 91.

(23) Krishnan, R.; Frisch, M. J.; Pople, J. A. *J. Chem. Phys.* **1980**, *72*, 4244..

(24) Pople, J. A.; Head-Gordon, M.; Raghavachari, K. *J. Chem. Phys.* **1987**, *87*, 5968.

(25) Frisch, M. J.; Trucks, G. W.; Schlegel, H. B.; Gill, P. M. W.; Johnson, B. J.; Robb, M. A.; Cheeseman, J. R.; Keith, T. A.; Petersson, G. A.; Montgomery, J. A.; Raghavachari, K.; Al-Laham, M. A.; Zakrzewski, V. G.; Ortiz, J. V.; Foresman, J. B.; Cioslowski, J.; Stefanov, B. B.; Nanayakkara, A.; Challacombe, M.; Peng, C. Y.; Ayala, P. Y.; Chen, W.; Wong, M. W.; Andres, J. L.; Replogle, E. S.; Gomperts, R.; Martin, R. L.; Fox, D. J.; Binkley, J. S.; DeFrees, D. J.; Baker, J.; Stewart, J. P.; Head-Gordon, M.; Gonzalez, C.; Pople, J. A. *Gaussian 94*; Gaussian, Inc.: Pittsburgh, PA, 1995.

(26) Bader, R. F. W. *Atoms in Molecules. A Quantum Theory*; Clarendon Press: Oxford, UK, 1990.

(27) Sudhakar, P. V.; Lammertsma, K. *J. Phys. Chem.* **1992**, *96*, 4830.

(28) del Río, E.; Barrientos, C.; Largo, A. *J. Phys. Chem.* **1996**, *100*, 14643.